

## General Disclaimer

### One or more of the Following Statements may affect this Document

- This document has been reproduced from the best copy furnished by the organizational source. It is being released in the interest of making available as much information as possible.
- This document may contain data, which exceeds the sheet parameters. It was furnished in this condition by the organizational source and is the best copy available.
- This document may contain tone-on-tone or color graphs, charts and/or pictures, which have been reproduced in black and white.
- This document is paginated as submitted by the original source.
- Portions of this document are not fully legible due to the historical nature of some of the material. However, it is the best reproduction available from the original submission.

82A 30118

NASA Technical Memorandum 82882

# Environmental and High-Strain Rate Effects on Composites for Engine Applications

(NASA-TM-82882) ENVIRONMENTAL AND HIGH-STRAIN RATE EFFECTS ON COMPOSITES FOR ENGINE APPLICATIONS (NASA) 20 p HC A02/MF A01

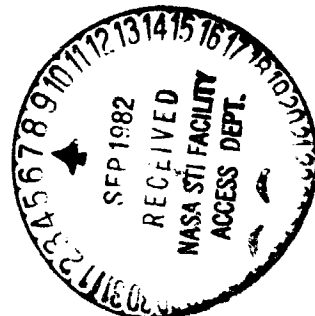
N82-31449

CSCI 11D

Unclass

H2/24 28855

C. C. Chamis and G. T. Smith  
*Lewis Research Center  
Cleveland, Ohio*



Prepared for the  
Twenty-third Structures, Structural Dynamics and Materials Conference  
cosponsored by the AIAA, ASME, ASCE, and AHS  
New Orleans, Louisiana, May 10-12, 1982



ENVIRONMENTAL AND HIGH STRAIN RATE EFFECTS  
ON COMPOSITES FOR ENGINE APPLICATIONS

C. C. Chamis\* and G. T. Smith\*\*

National Aeronautics and Space Administration  
Lewis Research Center  
Cleveland, Ohio 44135

Abstract

The Lewis Research Center is conducting a series of programs intended to investigate and develop the application of composite materials to structural components for turbojet engines. A significant part of that effort is directed to establishing the impact resistance, defect growth, and strain rate characteristics of composite materials over the wide range of environmental and load conditions found in commercial turbojet engine operations. Both analytical and experimental efforts are involved. This paper summarizes the status of the major experimental contract programs and attendant in-house and grant activities which include analytical methodology development.

Introduction

The complex environmental and loading conditions experienced by many turbine engine components impose severe durability and damage tolerance requirements for candidate component materials. These conditions include a wide spectrum of temperature and moisture as well as a variety of cyclic and impact loading situations. The programs conducted at Lewis are directed towards establishing the structural performance of composite materials under anticipated engine operating environments. Such programs require not only the measurement of composite material specimen response characteristics under appropriate combinations of loading, moisture and temperature, but also the development of analytical methods which can be used to analyze the detailed, local specimen response and to translate this performance of the composite material to the more complex engine component conditions. This paper describes experimental results obtained from several contract programs and attendant university grant and Lewis in-house programs which emphasize the analytical methodology developments.

Three contractual programs have been conducted which provide detailed data on the structural performance of composite materials under conditions that may be experienced in engine operation. The first program addressed the effects of hygrothermal and impact conditions on the structural performance of several graphite/epoxy and graphite/polyimide composites. Limited glass/epoxy data were also obtained. The second program examined the effects of moisture and temperature on the structural performance of graphite/epoxy materials containing stress concentrations and simulated natural defects. The third program determined the response of various graphite epoxy composite layups to very high-rate impact loading. In addition to these contractual programs, two Lewis/university grant programs are

\*Aerospace Structures and Composites Engineer, Member AIAA.

\*\*Aerospace Engineer.

involved. The first grant program is directed towards development of simple test and analytical models which can describe the energy absorbed by composites during impact loading. The second grant program was concerned with prediction of dynamic stress intensity factors in composites. The related Lewis Research Center in-house activities are concerned with development of simplified equations to predict the effects of hygrothermal environments on composite properties and on the continued development and implementation of the composite analysis program CODSTRAN (Composite Durability Structural Analysis).

### Comparison of Predicted and Measured Hygrothermal Effects

Hygrothermal effects on unidirectional composite properties (generated under contract)<sup>1</sup> were predicted using methods described in ref. 2. The predicted results were obtained from

$$\frac{P_h}{P_o} = \left[ \frac{T_{qw} - T}{T_{qd} - T_o} \right]^{1/2} \quad (1)$$

where  $P_h$  is the property with hygrothermal effects,  $P_o$  is the reference property,  $T_{qw}$  is the glass transition temperature of the wet composite,  $T_{qd}$  is the glass transition temperature of the composite at reference (nominally dry) moisture condition,  $T$  is the temperature at which  $P_h$  is needed, and  $T_o$  is the temperature at which the reference property  $P_o$  was determined. The equation can be used either at the ply level or at the composite micromechanics level using corresponding properties for the resin. The comparisons between measured data and predicted results of hygrothermal effects on composite flexural and interlaminar longitudinal and transverse strengths are shown in Fig. 1. The correlation between predicted and measured data is reasonable for both longitudinal and transverse flexural and interlaminar (short-beam-shear) strengths. Using the equation at the micromechanics level improves the correlation (solid square to solid diamond points) for longitudinal flexural strength. Using the degraded properties in laminate theory and in structural analysis of wedge type impact specimens shows that failure occurs earlier than it does in dry, room temperature conditions. The glass transition temperature of the wet composite ( $T_{qw}$ ) is not, in general, readily available. In the absence of experimental data,  $T_{qw}$  can be estimated from:

$$\left( \frac{T_{qw}}{T_{qd}} \right) = 0.01 m^2 - 0.10 m + 1.00 \quad (2)$$

where  $m$  is the weight percent moisture in the composite.

Equation (2) must be used judiciously and is limited to weight percent moistures of 5 or less and also to epoxy resins. A recommendation for determining moisture levels in composites for given mission conditions is illustrated in Fig. 2. Three essential points should be noted in Fig. 2: (1) The Kevlar composite absorbs considerably more moisture than either E-glass or T300 composites; (2) The constant condition exposure produces the highest moisture absorption in all three composites; and (3) The mission cycles exposure induces relatively small moisture absorption (about 0.5 percent) in the T300 composite.

The moisture profiles in Fig. 2 can be used with equations (2) and (1) to estimate composite property degradation due to hygrothermal environments. This procedure is illustrated using a specific example in the appendix.

### Hygrothermal Effects On Defect Growth

The hygrothermal effects on defect growth in composites were investigated using the specimen illustrated in Fig. 3 (ref 3). Typical results obtained are shown in Fig. 4 for an interply hybrid angleplied laminate  $(0/30/0^S/-30/0/30/0^S-30)_S$  (superscript s denotes S-glass/resin ply). This angleplied laminate is a candidate for fan blade applications for turbo-jet engines. The defects of the specimens of Fig. 4 consisted of centrally located through-the-thickness slots of length indicated by the defect size figure at the top of each bar. The comparisons show that there is a defect sensitivity effect at the room-temperature-dry and room-temperature-wet conditions between the smooth (without defect) and 1/8-in. slit. The defect sensitivity is less severe with increasing defect size and with elevated temperature. Data for other nonhybrid angleplied laminates show less defect sensitivity than that in Fig. 5 for the T300/Epoxy  $[0/+45/0/90]_S$  laminate and Fig. 6 for the T300/Epoxy  $[0_3/+90]_S$  laminate. The moisture, temperature, and defect size effects on the tensile strength of these materials as well as pertinent additional details of specimen fabrication and testing procedure can be found in ref. 3.

One remarkable conclusion from the data summarized in Figs. 4 to 6, is that both temperature and moisture have negligible or beneficial (room temperature wet) effects on the static tensile strength of composite laminates with crack-like defects. This conclusion is quite significant since the data are from three widely different laminate configurations including also one interply hybrid composite.

The hygrothermal effects on laminates with half-penetration defects, are shown in Fig. 7. The data in this figure show that the hygrothermal environment has negligible or beneficial effects on the static tensile strength. Another interesting observation from the data in Figs. 5 and 7 is that half penetration defects which are representative of surface defects and perhaps more severe, appear to have negligible effect on the static tensile strength of composite laminates. The hygrothermal effects on laminates with contour sunk holes are shown in Fig. 8. These effects are negligible or beneficial, for tensile static strength. Counter sunk holes in essence are larger-size defects. As such, they would cause greater static strength degradation than smooth hole defects. The data in Fig. 8 shows some degradation for the smaller-size defects at both room temperature-dry and room-temperature wet environmental conditions. However, the 300° F wet condition data shows negligible degradation. The important conclusions from the data in Figs. 7 and 8 are: (1) Hygrothermal environments have negligible effect on the static tensile strength of laminates with smooth and contour sunk hole-like defects; and (2) Hygrothermal environments tend to minimize, and even eliminate, the degradation effects of counter sinking on static tensile strength.

COUSTRAN (Composite Durability Structural Analysis)<sup>5</sup> is presently used at Lewis to model the defect growth and fracture of composites. Pilot model predicted results of a slotted specimen show that the same mechanical loading conditions induce more extensive damage in the presence of hygrothermal environments Fig. 9. Though COUSTRAN is not yet completely implemented, predicted results to date show that the defect growth and fracture in angleplied laminates can be simulated using concepts and procedures embedded in COUSTRAN.

## High Strain Rate Effects on Composite Mechanical Properties

The high-strain rate effects on composite mechanical properties were experimentally measured using a unique test method described in ref. 6 and illustrated in Fig. 10. A voluminous amount of dynamic data generated from this test method was acquired and reduced using a dedicated microprocessor. A typical stress/strain curve obtained from the reduced data is shown in Fig. 11. Moduli, Poisson's ratios, and fracture stresses and strains are obtained from these typical stress/strain curves.

The strain rate (dynamic) effects (about 150 in./in./sec) on initial transverse modulus are shown in Fig. 12 where the corresponding static values are also shown for comparison. The dynamic values are about three to four times greater than the static values. Comparable data for shear moduli are shown in Fig. 13. Strain rate has relatively small effect (less than 50 percent) on the shear moduli. Also, there appears to be some strain rate effect differences among the type of graphite fibers with the T300 fiber exhibiting the greatest increase in modulus.

The strain rate effects on transverse tensile strength are presented in Fig. 14. The dynamic strengths are about three to five times the static values. The strain rate effects on the transverse compression strength are shown in Fig. 15. The dynamic strengths are about one and one-half to two times the dynamic values. The strain rate effects on the intralaminar (in-plane) shear strength are shown in Fig. 16. The dynamic strengths differ from about 10 percent to 100 percent of the static values. The strain rate effects on the intralaminar shear strength is more pronounced for the T300/SP288 composite than for the AS/SP288 as was the case for the intralaminar shear modulus. Though data are not shown here, the strain rate effects on Poisson's ratios and fracture strains are negligible.

The very large increases in the transverse tensile strength coupled with an earlier Lewis investigation<sup>7</sup> on in situ ply strengths lead to an indication that in situ (in the angleplied laminate) transverse ply failure is an abrupt dynamic phenomenon occurring at high-strain rates. If this is indeed the case, then high-strain rate transverse tensile strength should be used in predicting angleplied laminate static strength based on first ply failure.

The above discussion indicates that the high strain rates (about 150 to 250 in./in./sec) have (1) Large effect (about three to five times) on transverse modulus and transverse tensile strength; (2) Substantial effect (about two times) on the transverse compressive strength; (3) Small effect on the intralaminar shear modulus and strength; (4) Negligible effect on Poisson's ratio and fracture strain; and (5) Dynamic transverse properties may be needed to determine first ply failure in the analysis of angleplied laminates.

## Dynamic Stress Intensity Factors in Composites

An analytical method and the requisite computer program was developed to determine the dynamic response of unidirectional composites containing flaws and subjected to off-axis (angle loading) impact (Fig. 17). The analytical method utilizes Fourier transform for the space variable and Laplace transform for the time variable. The off-axis impact is separated into two parts; one being symmetric and the other skew-symmetric with reference to the crack plane. Transient boundary conditions of normal and shear tractions are applied to a crack embedded in the matrix of the unidirectional composite. The two boundary conditions are solved independently and the results superimposed. Mathematically, these conditions reduce the problem to a system of

dual integral equations which are solved in the Laplace transform plane for the transform of the dynamic stress intensity factor. The time inversion is carried out numerically for various combinations of the material properties of the composite.

Typical results from this analytical method are shown in Fig. 18 for Mode II ( $K_2(t)$ ) dynamic stress intensity factor. The dynamic stress intensity factor,  $K_2(t)$ , is about 150 percent greater than its steady state value and occurs very early in the impact event. Analytical results for Mode I ( $K_1(t)$ ) are comparable to  $K_2(t)$ .<sup>8</sup> To the author's knowledge, this is the first analytical method available to determine the dynamic stress intensity factors for Modes I and II in fiber composites with cracks.

The high-strain rate effects on composite properties have not yet been incorporated in this analysis. It is anticipated that the magnitudes of both dynamic stress intensity factors  $K_1(t)$  and  $K_2(t)$  will be affected in view of the significant changes in the transverse modulus as described previously.

### Indentation Laws for Composite Impact Analysis

Experimental methods were developed to determine static indentation laws for fiber/epoxy laminates in contact with steel balls. The method is illustrated schematically in Fig. 19 and described in detail in ref. 9.

Static indentation tests were conducted on glass/epoxy and graphite/epoxy composite laminates with steel balls as the indenter. Beam specimens clamped at various spans were used for the tests. Loading, unloading, and reloading data were obtained and fitted into power laws. It was found that (1) indentation behavior is not appreciably affected by the specimen span; (2) Loading and reloading curves follow the 1.5 power law; and (3) unloading curves are described quite well by a 2.5 power law. Also values were found for the critical indentation,  $a_{cr}$ , which can be used to predict permanent indentations in unloading. Since  $a_{cr}$  only depends on composite material properties, only the loading and an unloading curve are sufficient to establish the complete loading-unloading-reloading behavior of composite laminates. A typical loading unloading record for a  $[0/45/0/-45/0]_{2s}$  graphite epoxy laminate is shown in Fig. 20. The equations describing the indentation laws are as follows:

Loading

$$F = K a^{1.5} \quad (3)$$

Unloading

$$F = F_m \left( \frac{a - a_0}{a_m - a_0} \right)^{2.5} \quad (4)$$

$$a_0 = a_m - \left( \frac{a_{cr}}{K} \right)^{0.4} F_m^{0.4} \quad (a_m \leq a_{cr}) \quad (5)$$

$$a_0 = 0 \quad (a_m > a_{cr})$$

The constants  $K_1$  and  $a_{cr}$  are determined from the indentation test;  $a_m$  is the indentation depth when unloading begins and  $F_m$  is the maximum force

ORIGINAL PAGE IS  
OF POOR QUALITY

ORIGINAL PAGE IS  
OF POOR QUALITY

prior to unloading. For a graphite/epoxy composite  $K = 5.94 \times 10^5$  lb/in.;  $a_{cr} = 3.2 \times 10^{-3}$  in.; values for  $a_m$  and  $F_m$  can be obtained from Fig. 20. For example,  $F_m$  is about 350 pounds and  $a_m$  is about  $4.7 \times 10^{-3}$  in. for the maximum unloading curve.

The above indentation laws were incorporated into a special transient finite element computer program developed for the impact analysis of beams. Predicted results and experimental data are plotted in Fig. 21. As can be seen, the predicted results are in very good agreement with the measured data. The important conclusion from the above discussion is that composite beam impact response can be accurately predicted with indentation laws determined using a relatively simple test method.

### Summary of Results

Significant results from the herein described research work on environmental and high strain rate effects on composites for engine applications include the following:

1. Simple equations (developed previously) accurately predict the hygrothermal effects in a variety of composite properties. Also a simple equation was developed to estimate the glass transition temperature of wet composites.
2. Hygrothermal environments have negligible effect on the static tensile strength of laminates with smooth and counter sunk hole-like defects.
3. Hygrothermal effects on defect growth and fracture of composites are realistically simulated using concepts embedded in CODSTRAN (Composite Durability Structural Analysis).
4. A unique test method was developed to measure high-strain rate effects. The method subjects thin rings to impulsive pressure loadings.
5. High strain rates (150 to 250 in./in./sec) have significant effects on composite transverse properties but have negligible effects on intralaminar shear properties.
6. An analytical method has been developed to predict dynamic stress intensity factors in off-axis loadings. The method predicts both Mode I ( $K_1(t)$ ) and Mode II ( $K_2(t)$ ) dynamic stress intensity factors. These factors are about 150 percent greater than their static values and occur very early in the impact event.
7. A simple test method has been developed, along with attendant indentation laws, for composite impact evaluation. These indentation laws, coupled with finite element transient analysis, predict the impact response of a fixed beam which is in very good agreement with measured data.

### References

1. Murphy, G. C. and Selemme, C. T., "Environmental Effects on FOD Resistance of Composite Fan Blades," General Electric Co., Cincinnati, OH RB1AEG094, Jan. 1981. (NASA CR-165211).
2. Porter, T. R., "Evaluation of Flawed Composite Structural Components Under Static and Cyclic Loading - fatigue life of graphite epoxy composite materials," Boeing Aerospace Co., Seattle, WA, NAS3-19709, Feb. 1979. (NASA CR-135404).
3. Chamis, C. C., Lark, R. F., and Sinclair, J. H., "An Integrated Theory for Predicting the Hygrothermomechanical Response of Advanced Composite Structural Components," NASA TM-73812, 1977.



4. Chamis, C. C., and Smith, G. T., "Engine Environmental Effects on Composite Behavior," NASA TM-81508, 1980.
5. Chamis, C. C., and Smith, G. T., "CODSTRAN: Composite Durability Structural Analysis," NASA TM-79070, 1978.
6. Daniel, I. M., LaBedz, R. H., and Liber, T., "New Method for Testing Composites at Very High Strain Rates", Experimental Mechanics, Vol. 21, No. 2, Feb. 1981, pp 71-77
7. Chamis, C. C., and Sullivan, T. L., "In Situ Ply Strength: An Initial Assessment - using laminate fracture data and a least squares method," NASA TM-73771, 1978.
8. Sih, G. C. , and Chen, E. P., "Off-Axis Impact of Unidirectional Composites with Cracks: Dynamic Stress Intensification," Lehigh Univ., Bethlehem, PA, IFSM-79-95, Jan. 1979. (NASA CR-159537).
9. Sun, C. T., and Yang, S. H., "Contact Law and Impact Responses of Laminated Composites," Purdue Univ., Lafayette, IN, CML-80-1. Feb. 1980. (NASA CR-159884).

APPENDIX - ESTIMATION OF PROPERTY DEGRADATION  
IN HYGROTHERMAL ENVIRONMENTS

Estimate the hygrothermally degraded properties of Kevlar, E-glass and T300 epoxy composites when these composites are subjected to multiple mission cycles exposures and 200° F. The moisture contents in the composite at the end of 10 cycles are: 2.5 percent for Kevlar, 0.7 percent for E-glass and 0.5 percent for T300. The glass transition temperature of the dry composite ( $T_{gd}$ ) equals 430° F. The use temperature ( $T$ ) equals 200° F. The reference temperature ( $T_0$ ) is 70° F (room temperature). The glass transition temperature of the wet composite ( $T_{gw}$ ) is estimated from equation (2). Using the moisture contents for the respective composites in equation (2), the corresponding  $T_{gw}$ 's are 349° F for Kevlar, 402° F for E-glass and 410° F for T300. Using these  $T_{gw}$ 's together with  $T_{gd}$  and  $T$  in equation (1), the corresponding degraded properties ratio ( $P/P_0$ ) is 0.414 for Kevlar, 0.561 for E-glass and 0.583 for T300. The degraded property ratio applies only to resin control composite properties such as flexural, compressive, transverse, intralaminar and interlaminar shear properties.

ORIGINAL PAGE IS  
OF POOR QUALITY

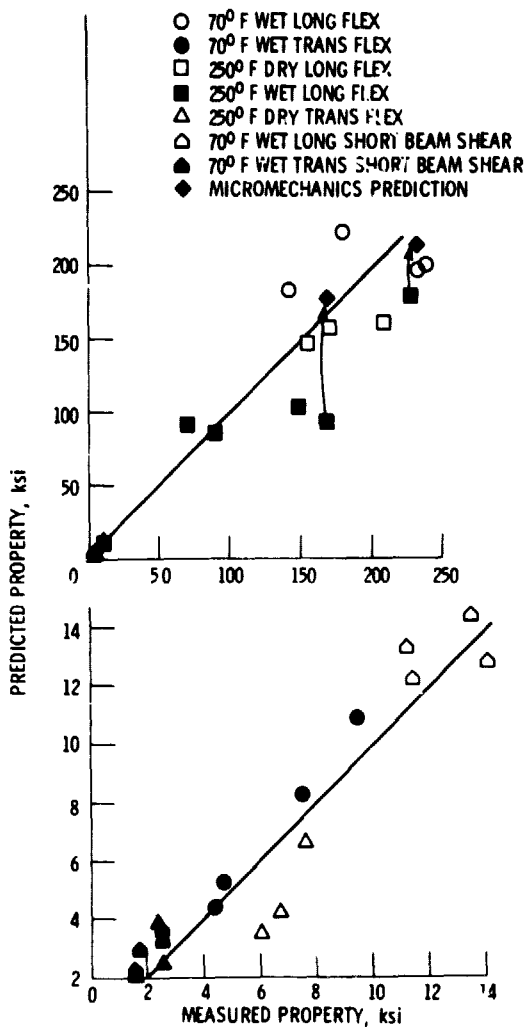
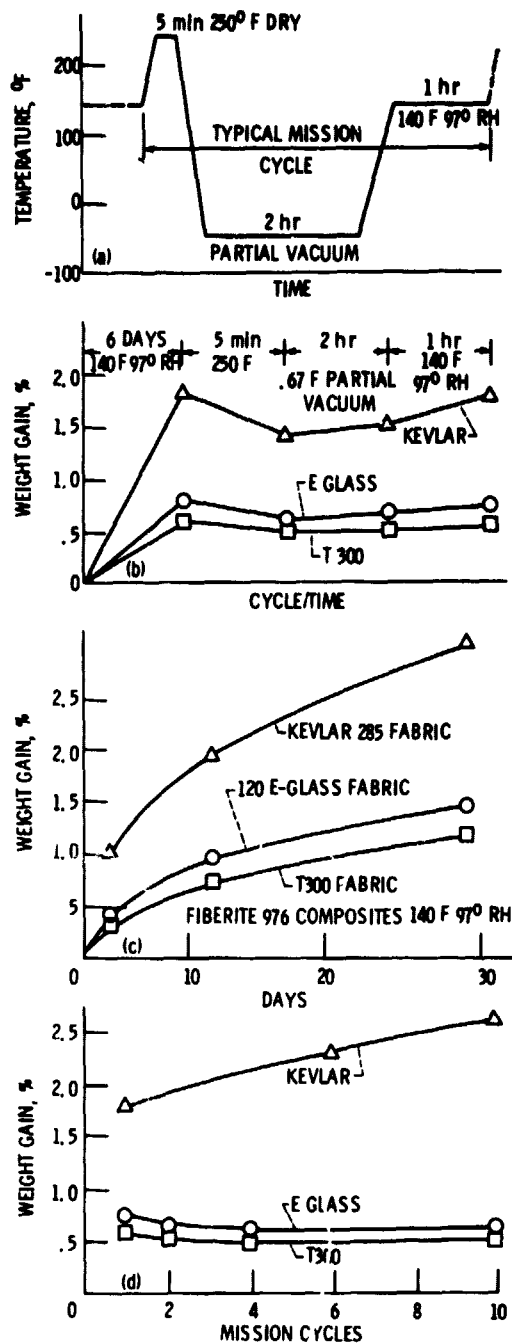


Figure 1. - Comparison of predicted and measured hygrothermal effects on mechanical properties of composite materials.



- (a) Determine mission conditions.
- (b) Moisture migration during mission cycle.
- (c) Effect of constant conditions.
- (d) Moisture stabilization after multiple mission cycles.

Figure 2. - Determination of operational moisture content of composite material structural components.

ORIGINAL PAGE IS  
OF POOR QUALITY

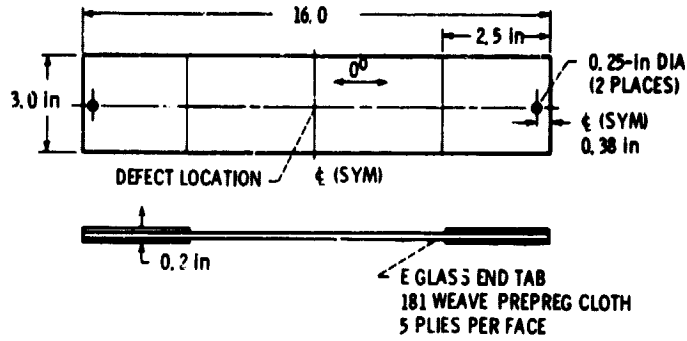
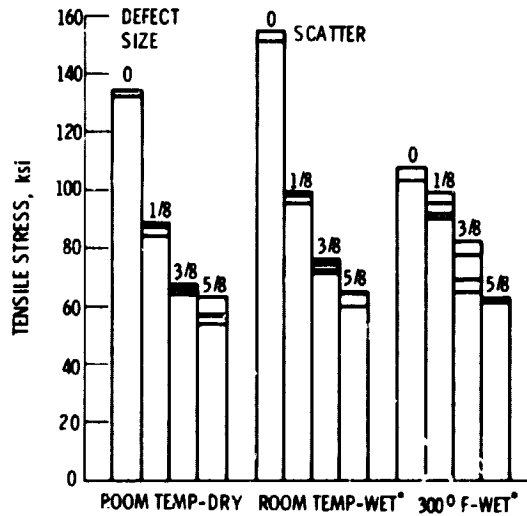


Figure 3. - Specimen configuration for evaluation of defect size, moisture content and temperature level on the tensile strength of T-300/epoxy.



\* WET  $\approx$  1.9% MOISTURE

Figure 4. - Defect size and hygrothermal effects on composite tensile strength (T-300/epoxy [0/30/0<sup>5</sup>/-30/0/30/0<sup>5</sup>/-30]<sub>S</sub>, 0<sup>5</sup> denotes 0° S-glass/epoxy.

ORIGINAL PAGE IS  
OF POOR QUALITY

T-300/EPOXY;  $[0/\pm 45/90]_5$

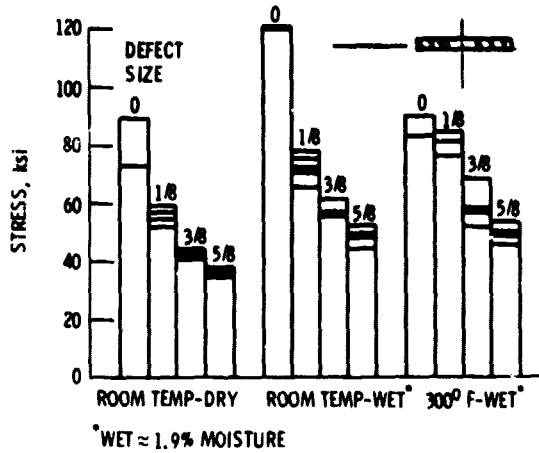


Figure 5. - Defect size and hygrothermal effects on tensile strength of general purpose structural composite.

T-300/EPOXY;  $[0_3/\pm 80]_{25}$

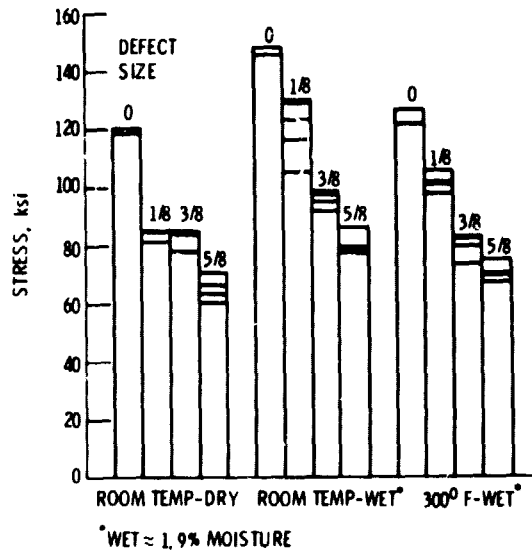


Figure 6. - Defect size and hygrothermal effects on tensile strength of a pressure vessel overwrap composite.

ORIGINAL PAGE IS  
OF POOR QUALITY

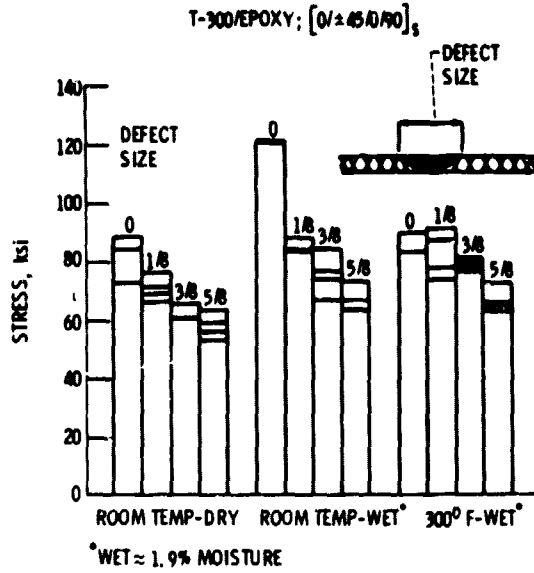


Figure 7. - Half penetration defect size and hygrothermal effects on tensile strength of general purpose structural composite.

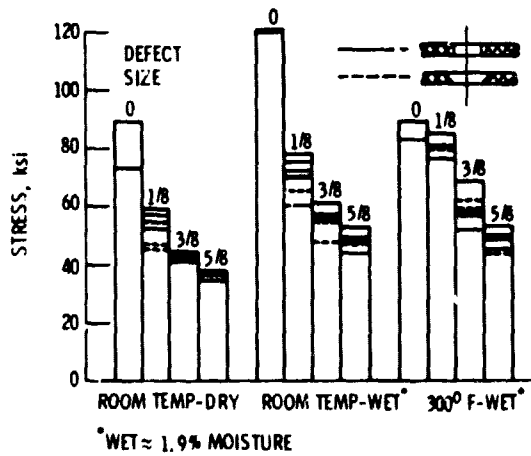


Figure 8 - Comparison of full penetration and over-countersunk holes on the tensile strengths of T-300/EPOXY [0/±45/90]<sub>s</sub> composite materials.

ORIGINAL PAGE IS  
OF POOR QUALITY

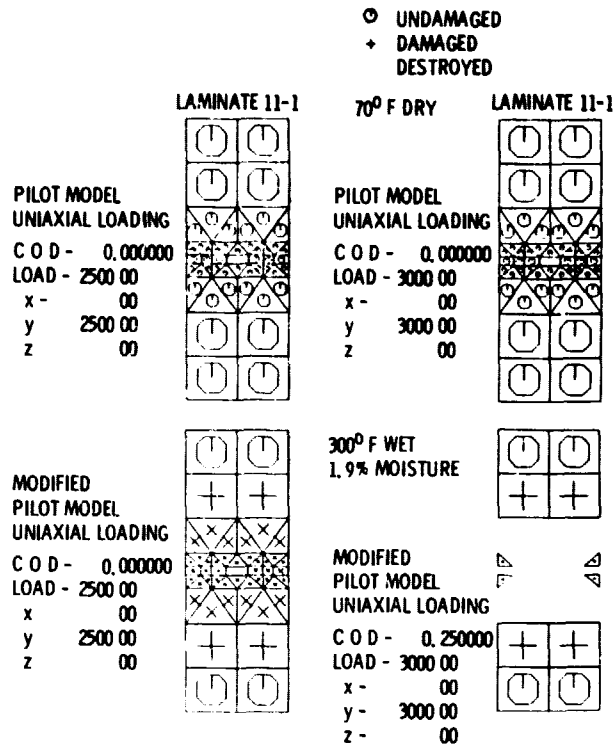


Figure 9. - Effect of load, temperature, and moisture on damage growth in T-300/epoxy  $[0/\pm 30/\mp 30/0]_S$ .

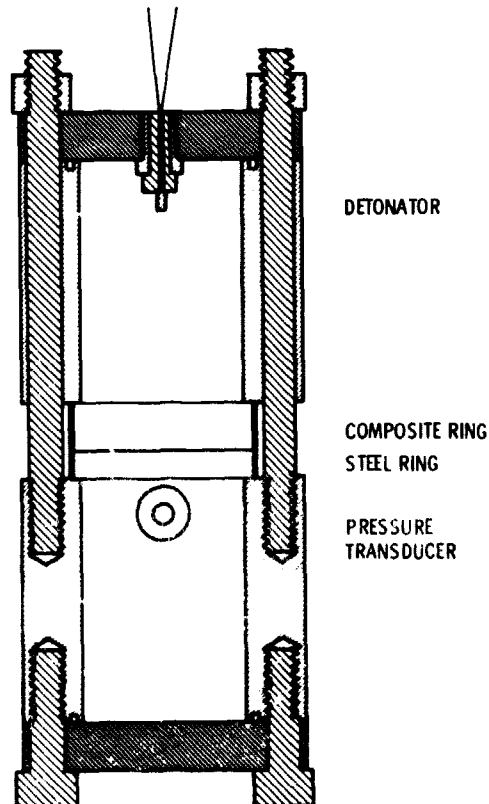


Figure 10. - Fixture for dynamic loading composite ring specimens.

ORIGINAL PAGE IS  
OF POOR QUALITY

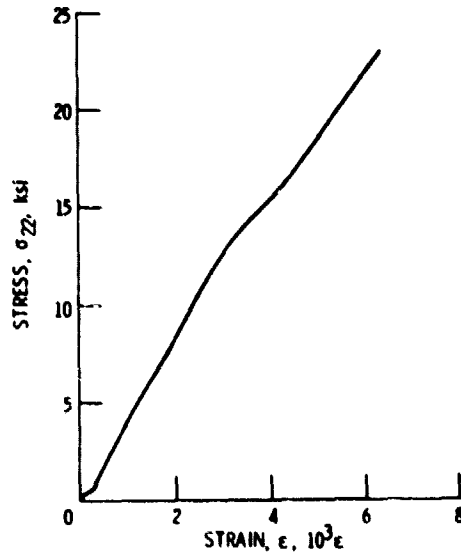


Figure 11. - Stress-strain curve for dynamically loaded  $[90]_{\theta}$  SP288/AS graphite/epoxy ring.

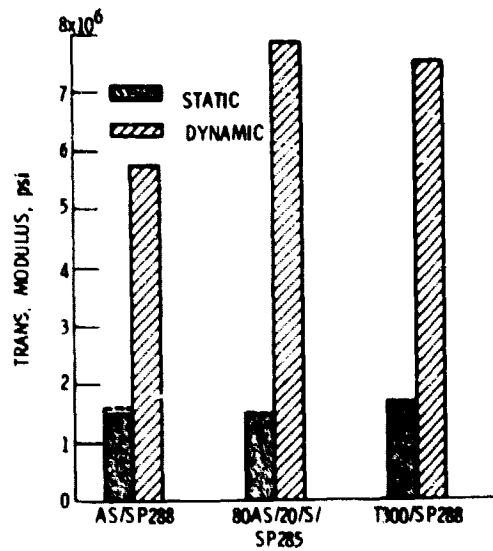


Figure 12. - Effect of high strain rate on initial transverse modulus of graphite/epoxy composites at 150 in/in/sec (room temperature dry).



ORIGINAL PAGE IS  
OF POOR QUALITY

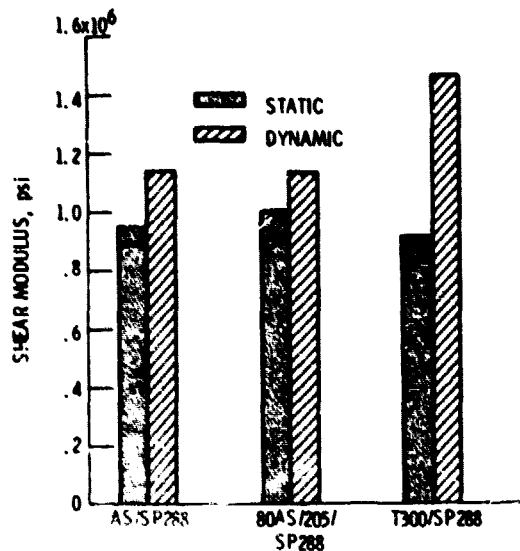


Figure 13 - Effect of high strain rate on initial shear modulus of graphite/epoxy composites at 150 in/in/sec (room temperature dry).

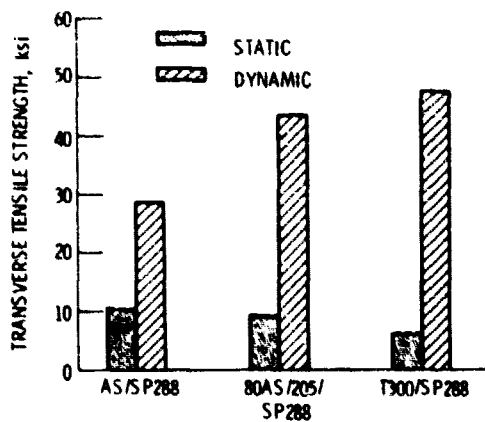


Figure 14 - Effect of high strain rate on the transverse tensile strength of graphite/epoxy at 150 in/in/sec (room temperature dry).

ORIGINAL PAGE IS  
OF POOR QUALITY

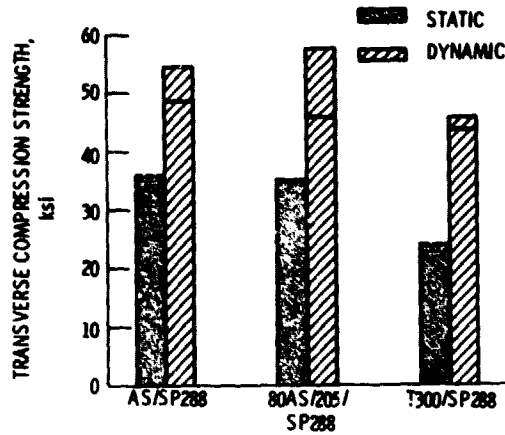


Figure 15. - Effect of high strain rate on the transverse compression strength of graphite/epoxy at 150 in/in/sec (room temperature dry).

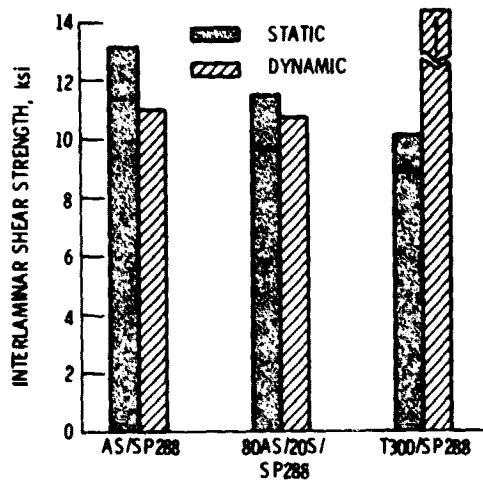


Figure 16. - Effect of high strain rate on the interlaminar shear strength of graphite/epoxy at 150 in/in/sec (room temperature dry).

ORIGINAL PAGE IS  
OF POOR QUALITY

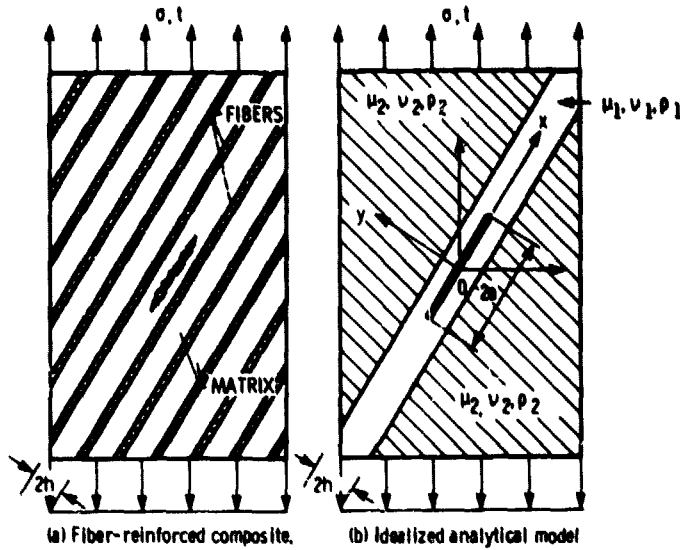


Figure 17. - Fiber-reinforced unidirectional composite subjected to angle impact loading.

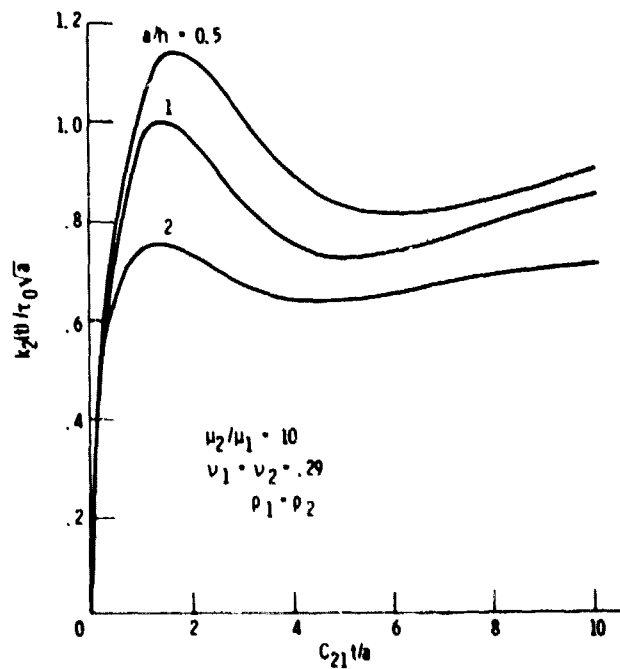


Figure 18. - In plane shear stress intensity factor response due to impact rate loading conditions (see fig. 17 for geometry and notation).

ORIGINAL PAGE IS  
OF POOR QUALITY

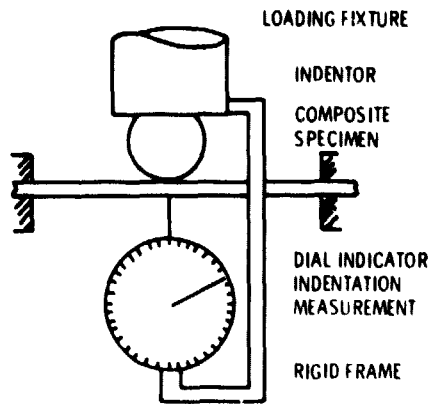


Figure 19. - Indentation test for compact specimen.

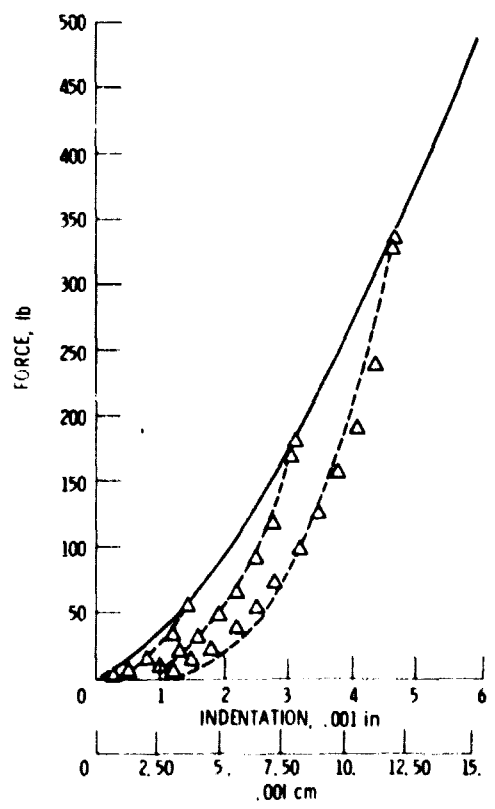


Figure 20. - Loading and unloading curves for a graphite/epoxy  $(N/45/D-45/D)_2$  laminate.

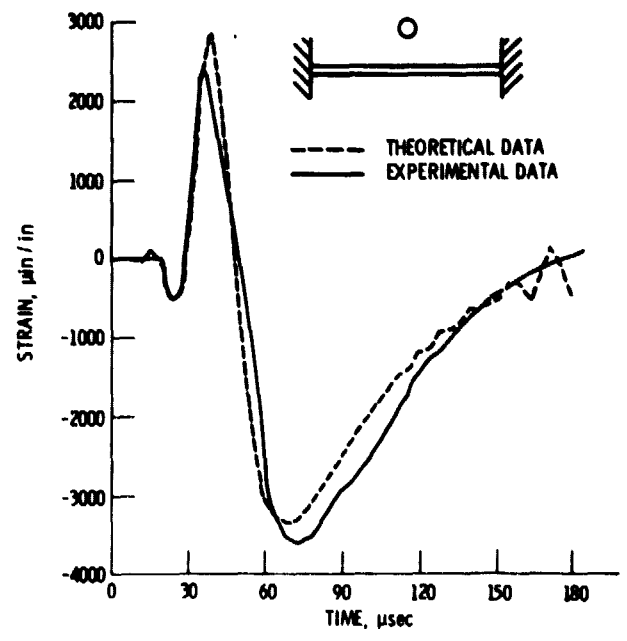


Figure 21. - Comparison of experimental and predicted bending strain response of composite beam impacted at about 1200 in/sec.